Complex Gyrator Circuits of Planar Circulators Using Higher Order Modes in a Disk Resonator

J. HELSZAJN, MEMBER, IEEE

Abstract—**The use of resonators or waveguides utilizing higher order modes is often an attractive solution to the design of millimeter microwave networks. This paper investigates the complex gyrator circuit of a planar junction circulator employing higher order solutions in a disk resonator. The first such solution displays many of the features of weakly magnetized junctions using the dominant mode in a disk resonator, but its loaded Q-factor is incompatible with the realization of quarter-wave coupled devices. Although the second one exhibits more useful equivalent circuits, it requires a relatively large magnetization, which is not altogether practical at millimeter frequencies. A circulator configuration that has a frequency response akin to that of a quarter-wave coupled one is one where the in-phase eigennetwork is degenerate with those of the demagnetized counter-rotating eigennetworks. The degeneracy between the in-phase limit, $TM_{2,0,-2}$, and the second-order counter-rotating limit, $TM_{1,1,-2}$ modes, in an oversized irregular hexagonal resonator, is used in this paper to construct such a device.**

I. Introduction

ONE MODEL of a junction circulator is in terms of a symmetrically magnetized ferrite resonator symmetrically coupled by three transmission lines. Although the lowest order mode in the resonator is usually employed in circulator design, the possibility of using higher solutions is also well understood [1]–[3]. The purpose of this paper is to determine the complex gyrator circuit and network problem of such a junction using a simple disk resonator in terms of its gyrator conductance (G), susceptance slope parameter (B'), and loaded Q-factor (Q_L). These solutions are defined with the off-diagonal element of the tensor permeability (κ) in the interval $0 \leqslant \kappa \leqslant 0.40$ and $0.40 \leqslant \kappa \leqslant 0.80$. In the vicinity of the origin, for very weakly magnetized resonators, the relationships between the coupling angle (ψ), the off-diagonal entry of the tensor permeability (κ), and the loaded Q-factor (Q_L) conform to that of the dominant solution [4]. The main difference between them is that whereas the complex gyrator circuit of the dominant mode can be adjusted to exhibit a wide range of loaded Q-factors, this circuit has a minimum value for this quantity of about 12. Examination of the network problem [5]–[7] indicates that such a value of loaded Q-factor is incompatible with the synthesis of quarter-wave coupled devices. However, the second higher order solution exhibits equivalent circuits and values of loaded Q-factor that are suitable for the synthesis of quarter-wave coupled junction circulators with modest specifications.

A circuit topology that has a frequency response akin to that realizable with a single quarter-wave transformer is obtained by resonating the usually nonresonant in-phase mode in some way to the degenerate counter-rotating ones or by seeking some natural degeneracy between them [8]–[11]. One such degeneracy between a pair of second higher order modes and an in-phase one is in fact encountered in an irregular hexagonal resonator [12]. This paper includes the experimental development of such a circulator and the derivation of the network problem.

II. Complex Gyrator Circuit

The frequency response of the dominant circulation solution of a junction circulator using a disk resonator is usually formed by describing the eigennetworks of the junction in terms of the first seven resonator modes. The schematic diagram of the junction discussed here is depicted in Figs. 1 and 2. To cater to the proximity of the $n = \pm 4$ modes to the $n = \pm 2$ ones, these are included in the description of the boundary conditions

$$Z^0 \approx Z_0 + Z_{+3} + Z_{-3} \tag{1}$$

$$Z^+ \approx Z_{+1} + Z_{-2} + Z_{+4} \tag{2}$$

$$Z^- \approx Z_{-1} + Z_{+2} + Z_{-4}. \tag{3}$$

The poles Z_n of the eigenvalues Z^0, Z^+, and Z^- have the usual form given in [13]. The corresponding eigennetworks are illustrated in Fig. 3.

The complex gyrator impedance of the junction at port 1 obtained by decoupling port 3 from port 2 is

$$Z_{\text{in}} = R + jX = Z_{11} - \frac{Z_{12}^2}{Z_{13}} \tag{4}$$

and the complex gyrator admittance is given by

$$Y_{\text{in}} = \frac{1}{Z_{\text{in}}} = G + jB. \tag{5}$$

The relationships between the eigenvalues Z^0, Z^+, and Z^- and the open-circuited parameters Z_{11}, Z_{12}, and Z_{13} are

Manuscript received December 29, 1982; revised June 1, 1983.

The author is with Department of Electrical Heriot-Watt University and Electronic Engineering, 31-35 Grassmarket, Edinburgh EH1 2HT, Scotland.

0018-9480/83/1100-0931$01.00 ©1983 IEEE

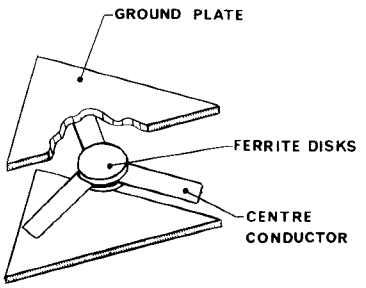

Fig. 1. Schematic diagram of stripline circulator using a disk resonator.

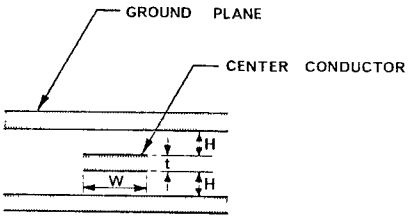

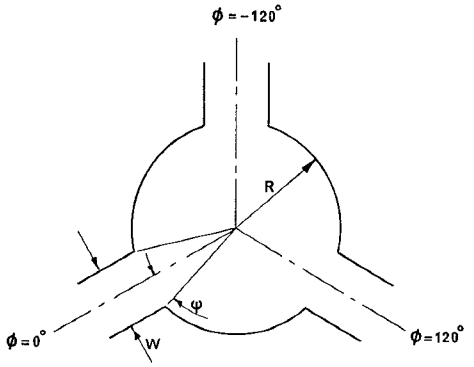

Fig. 2. Physical variables of stripline circulator using a disk resonator.

also given in [13] and elsewhere by

$$Z_{11} = \frac{Z^0 + Z^+ + Z^-}{3} \tag{6}$$

$$Z_{12} = \frac{Z^0 + Z^+ \exp(jn2\pi/3) + Z^- \exp(-j2n\pi/3)}{3} \tag{7}$$

$$Z_{13} = \frac{Z^0 + Z^+ \exp(-jn2\pi/3) + Z^- \exp(j2\pi n/3)}{3}. \tag{8}$$

n is taken as 2 for the second-order solution.

The one-port complex gyrator circuit is completely determined by its gyrator conductance (G), its susceptance slope parameter (B'), and by its loaded Q-factor (Q_L). The planar circuit is defined by the coupling angle (ψ), the off-diagonal element of the tensor permeability (κ), and by the wavenumber (kR). The variables in the physical problem are

$$\sin\psi = \frac{W}{2R} \tag{9}$$

$$k = \frac{2\pi}{\lambda_0}\sqrt{\epsilon_f \mu_{\text{eff}}} \tag{10}$$

$$Y_f = \sqrt{\epsilon_f}\, Y_r \tag{11}$$

$$Y_r = \left[30\pi \ln \frac{(W+2H+t)}{W+t}\right]^{-1}. \tag{12}$$

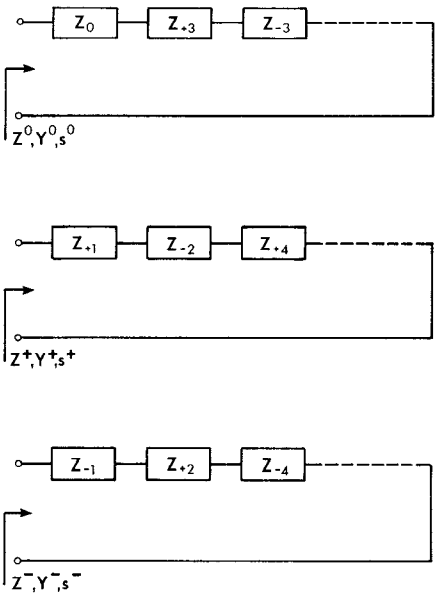

Fig 3. Eigennetworks of three-port junction circulators.

For a saturated material

$$\mu_{\text{eff}} = 1 - \kappa^2 \tag{13}$$

$$\mu = 1 \tag{14}$$

$$\kappa = \frac{\gamma M_0}{\mu_0 \omega}. \tag{15}$$

γ is the gyromagnetic ratio (2.21×10^5 (rad/s)/(A/m)), M_0 is the saturation magnetization (T), μ_0 is the free-space permeability ($4\pi \times 10^{-7}$ H/m), ω is the radian frequency (rad/s), λ_0 is the free-space wavelength (m), and ϵ_f is the relative dielectric constant of the ferrite material.

III. Second-Mode Circulation Solution

Table I displays the complete second-order circulation solution for κ between 0 and 0.40 and psi equal to 0.10, 0.20, 0.30, and 0.35. It is defined by the interval $0 \leqslant \kappa \leqslant 0.40$, and this is the range tabulated here [1], [3]. In this interval, the gyrator conductance increases from 0 at $\kappa = 0$ to some maximum value, and then decreases back to zero at κ, approximately equal to 0.40. The negative gyrator conductance exhibited by the circuit merely implies that this mode circulates in the opposite direction to that of the dominant one. Outside this range, the direction of circulation reverses. The variation of G in these tables has the nature of the data in [1], [3]. The relationship between the loaded Q-factor and the magnetic variables follow directly from that of the gyrator variable. This quantity exhibits a minimum value (approximately 12) at the magnetic state where the gyrator conductance is a maximum. Closed-form solutions may be derived in the vicinity of the origin by writing (1) thru (3) as

$$Z^0 \approx 0 \tag{16}$$

$$Z^+ \approx Z_{+2} \tag{17}$$

$$Z^- \approx Z_{-2} \tag{18}$$

and the two circulation conditions obtained by setting

TABLE I

κ	kR	G	B'	Q
0.025	3.0619	-0.0085	0.2731	32.2507
0.050	3.0825	-0.0160	0.2893	18.1305
0.075	3.1115	-0.0220	0.3097	14.0565
0.100	3.1449	-0.0267	0.3306	12.3734
0.125	3.1800	-0.0302	0.3505	11.6082
0.150	3.2152	-0.0327	0.3692	11.3075
0.175	3.2497	-0.0342	0.3869	11.3000
0.200	3.2829	-0.0350	0.4035	11.5197
0.225	3.3143	-0.0351	0.4190	11.9519
0.250	3.3438	-0.0343	0.4332	12.6195
0.275	3.3710	-0.0327	0.4451	13.5923
0.300	3.3957	-0.0302	0.4538	15.0253
0.325	3.4172	-0.0264	0.4568	17.2870
0.350	3.4347	-0.0211	0.4512	21.4337
0.375	3.4460	-0.0135	0.4322	32.0380
0.400	3.4476	-0.0032	0.3973	123.3907

ψ = 0.3

κ	kR	G	B'	Q
0.025	3.0624	-0.0228	0.7355	32.2757
0.050	3.0842	-0.0429	0.7794	18.1650
0.075	3.1147	-0.0592	0.8339	14.0903
0.100	3.1494	-0.0717	0.8892	12.4037
0.125	3.1856	-0.0809	0.9421	11.6395
0.150	3.2215	-0.0874	0.9918	11.3478
0.175	3.2562	-0.0914	1.0388	11.3605
0.200	3.2892	-0.0933	1.0834	11.6138
0.225	3.3201	-0.0930	1.1252	12.0958
0.250	3.3487	-0.0906	1.1630	12.8348
0.275	3.3748	-0.0859	1.1948	13.9084
0.300	3.3981	-0.0785	1.2165	15.4877
0.325	3.4182	-0.0680	1.2221	17.9717
0.350	3.4343	-0.0534	1.2024	22.4979
0.375	3.4448	-0.0337	1.1446	33.9263
0.400	3.4471	-0.0080	1.0406	130.6242

ψ = 0.1

κ	kR	G	B'	Q
0.025	3.0617	-0.0076	0.2447	32.2367
0.050	3.0818	-0.0143	0.2591	18.1083
0.075	3.1103	-0.0198	0.2774	14.0321
0.100	3.1432	-0.0240	0.2962	12.3487
0.125	3.1779	-0.0271	0.3142	11.5827
0.150	3.2129	-0.0294	0.3311	11.2783
0.175	3.2473	-0.0308	0.3470	11.2635
0.200	3.2804	-0.0316	0.3620	11.4711
0.225	3.3121	-0.0316	0.3760	11.8844
0.250	3.3418	-0.0310	0.3887	12.5253
0.275	3.3695	-0.0297	0.3997	13.4589
0.300	3.3947	-0.0275	0.4076	14.8345
0.325	3.4168	-0.0242	0.4108	17.0073
0.350	3.4348	-0.0193	0.4062	21.0052
0.375	3.4466	-0.0125	0.3905	31.2772
0.400	3.4479	-0.0030	0.3610	120.4850

ψ = 0.35

κ	kR	G	B'	Q
0.025	3.0622	-0.0119	0.3828	32.2691
0.050	3.0835	-0.0223	0.4056	18.1557
0.075	3.1135	-0.0308	0.4342	14.0831
0.100	3.1477	-0.0374	0.4632	12.3985
0.125	3.1834	-0.0422	0.4908	11.6341
0.150	3.2190	-0.0456	0.5168	11.3389
0.175	3.2537	-0.0477	0.5414	11.3437
0.200	3.2868	-0.0487	0.5646	11.5838
0.225	3.3179	-0.0487	0.5863	12.0465
0.250	3.3469	-0.0475	0.6061	12.7580
0.275	3.3734	-0.0451	0.6226	13.7929
0.300	3.3972	-0.0414	0.6342	15.3165
0.325	3.4179	-0.0360	0.6377	17.7154
0.350	3.4344	-0.0284	0.6280	22.1004
0.375	2.4453	-0.0181	0.5995	33.2012
0.400	3.4473	-0.0043	0.5469	127.7411

ψ = 0.2

$B = 0$ (or $X = 0$) and evaluating G(or R) are given by

$$G = \frac{4\pi Y_f}{\sqrt{3}\sqrt{\mu_{\text{eff}}}(kR)\sin 2\psi}\frac{\kappa}{\mu} \tag{19}$$

$$B = \frac{2\pi Y_f}{3\sqrt{\mu_{\text{eff}}}\sin 2\psi}\left[\frac{J_2'(kR)}{J_2(kR)}\right]. \tag{20}$$

The susceptance slope parameter and loaded Q-factor are readily evaluated in terms of the preceding equations as

$$B' = \frac{\pi Y_f}{3\sqrt{\mu_{\text{eff}}}\sin 2\psi}\left[\frac{(kR)^2-4}{kR}\right] \tag{21}$$

$$Q_L = \left[\frac{(kR)^2-4}{4\sqrt{3}}\right]\frac{\mu}{\kappa}. \tag{22}$$

The resonant frequency is determined by

$$J_2'(kR) = 0 \tag{23}$$

or

$$kR = 3.04. \tag{24}$$

The approximate closed-form solutions given here are in keeping with the numerical data in Table I for κ between 0 and 0.075.

In addition to the network description of the complex gyrator circuit, it is also necessary to verify that its frequency response is compatible with its loaded Q-factor. Fig. 4 illustrates one typical response. Although these circuits are not, in general, particularly well behaved over an extended frequency interval, a more serious shortcoming of these solutions is that the loaded Q-factors exhibited by them lead to unrealizable impedance levels for the junctions. Taking the case illustrated in Fig. 4 in conjunction with a single transformer circuit, as an example, gives

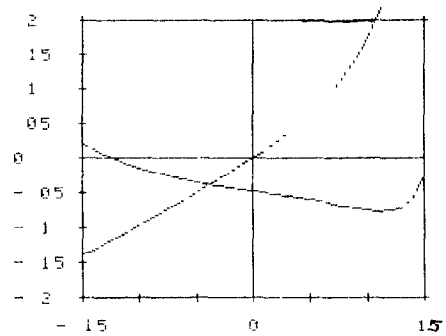

Fig. 4. Frequency response of complex gyrator circuit for first higher order circulation solution with $\kappa = 0.175$, $\psi = 0.020$, and $kR = 3.2537$.

the following variables for the network problem [7]:

$$Q_L = 11.344$$
$$S(\min) = 1.05$$
$$S(\max) = 1.20$$
$$W = 0.058$$
$$G = 2.769 \text{ (S)}$$
$$Y_r = 1.161 \text{ (S)}.$$

The value of Y_r required here is obviously incompatible with good engineering practice.

$S(\min)$ and $S(\max)$ are the minimum and maximum values of the VSWR, and W is the normalized bandwidth.

IV. Third-Mode Circulation Solution

The third circulation solution in a junction circulator using a disk resonator is defined with the magnetic variable κ in the interval $0.40 \lesssim \kappa \lesssim 0.80$. Over a limited combination of the variables κ, ψ, and kR, this solution, unlike the second-order one, exhibits some useful equivalent circuits and values of loaded Q-factor for the synthesis of quarter-wave coupled devices. The direction of circulation of this mode is the opposite sense to that of the second-order mode. Table II depicts some typical results. The range of values of loaded Q-factors exhibited by this solution is appropriate for the synthesis of quarter-wave coupled devices with modest specifications. Although the frequency responses of all these circuits are not particularly well behaved, some useful solutions are to be located within this field. One such solution is illustrated in Fig. 5. Taking this result as an example leads to the following network problem:

$$Q = 2.093$$
$$S(\min) = 1.060$$
$$S(\max) = 1.100$$
$$W = 0.193$$
$$G = 0.119 \text{ (S)}$$
$$Y_r = 0.048 \text{ (S)}.$$

This network solution exhibits a more useful bandwidth (W) and an acceptable admittance level (Y_r). However, the required normalized magnetization is somewhat on the large side to be useful as millimeter frequencies.

Fig. 6 illustrates the relationship between Q_L and κ for $\psi = 0.35$ for the first two higher order circulation solutions.

V. Synthesis of Junction Circulators Using Resonant In-Phase Eigennetworks

The in-phase eigennetwork of a three-port junction circulator may often be idealized by a frequency-independent short-circuit boundary condition at its input terminals, but may also be adjusted to either exhibit a series or shunt resonance there [8]–[11]. The synthesis of the former problem is well understood, but only one of the latter cases has been described in the literature [11]. The two eigenvalue diagrams applicable here are illustrated in Figs. 7(a) and (b). The equivalent circuit exhibited by the data in Tables I and II is an example of the former situation. Approximate equivalent circuits for the latter two situations may be readily realized from a knowledge of their complex gyrator immittances. In the case for which $s_0 = -1$, it is appropriate to employ open-circuit parameters in forming the complex gyrator immittance. The result is [13]

$$Z_{\text{in}} \approx \frac{8Z^0 - (Z^+ + Z^-)}{6} + j\frac{(Z^+ - Z^-)}{2\sqrt{3}}. \tag{25}$$

In obtaining this result, the in-phase eigenvalue Z^0 has been idealized by a short-circuit boundary condition in forming the real part of the gyrator immittance. This impedance is readily realized in the form indicated in Fig. 8 by writing Z_{in} as

$$Z_{\text{in}} = Z_1 + \frac{1}{Y_1} \tag{26}$$

where

$$Z_1 \approx \frac{4Z^0}{3} \tag{27}$$

$$Y_1 \approx \frac{(Y^+ + Y^-)}{2} + j\sqrt{3}\,\frac{(Y^+ - Y^-)}{2}. \tag{28}$$

An equivalent result has been derived in [11] in terms of the reflection scattering variable S_{11} and its derivative, but the approach used here is more straightforward. The equivalent circuit in Fig. 8 reduces to the usual approximation by omitting the Z^0 term in the previous derivation. This circuit has the nature of a bandpass filter which may be adjusted to display a reflection or transmission characteristic akin to that of a quarter-wave coupled junction with its in-phase eigennetwork idealized by a short-circuit boundary condition (see below).

The realization of the gyrator circuit of a junction in the situation where the in-phase eigennetwork exhibits a shunt resonance at its terminals ($s_0 = +1$) proceeds in a dual fashion to the preceding case except that short-circuit, instead of open-circuit, parameters are employed.

$$Y_{\text{in}} \approx \frac{8Y^0 - (Y^+ + Y^-)}{6} + j\frac{(Y^+ - Y^-)}{2\sqrt{3}}. \tag{29}$$

This admittance may be synthesized in the form illustrated in Fig. 9 by expressing Y_{in} as

$$Y_{\text{in}} = Y_1 + \frac{1}{Z_1} \tag{30}$$

TABLE II

K	KR	G	B'	Q
0.4075	3.4454	0.0004	0.3841	970.6861
0.4250	3.4337	0.0095	0.3503	36.7044
0.4500	3.3992	0.0228	0.3018	13.2205
0.4750	3.3445	0.0341	0.2595	7.6174
0.5000	3.2744	0.0423	0.2251	5.3248
0.5250	3.1935	0.0478	0.1976	4.1346
0.5500	3.1051	0.0514	0.1758	3.4239
0.5750	3.0112	0.0534	0.1582	2.9596
0.6000	2.9131	0.0544	0.1437	2.6419
0.6250	2.8114	0.0543	0.1319	2.4270
0.6500	2.7066	0.0531	0.1227	2.3100
0.6750	2.5995	0.0503	0.1180	2.3449
0.7000	2.4922	0.0447	0.1250	2.7980
0.7250	2.3918	0.0335	0.1800	5.3776
0.7500	2.3192	0.0131	0.4494	34.3185
0.7625	2.3006	0.0007	0.7629	1111.6253

ψ = 0.3

K	KR	G	B'	Q
0.4075	3.4453	0.0004	0.3499	939.3312
0.4250	3.4325	0.0089	0.3220	36.2844
0.4500	3.3957	0.0212	0.2815	13.3030
0.4750	3.3387	0.0315	0.2436	7.7229
0.5000	3.2664	0.0392	0.2102	5.3620
0.5250	3.1833	0.0445	0.1824	4.1012
0.5500	3.0927	0.0480	0.1600	3.3372
0.5750	2.9966	0.0501	0.1421	2.8372
0.6000	2.8965	0.0511	0.1278	2.5019
0.6250	2.7933	0.0511	0.1170	2.2908
0.6500	2.6880	0.0499	0.1102	2.2108
0.6750	2.5822	0.0470	0.1102	2.3471
0.7000	2.4790	0.0412	0.1258	3.0521
0.7250	2.3863	0.0303	0.1892	6.2407
0.7500	2.3195	0.0119	0.4121	34.6862
0.7625	2.3007	0.0006	0.6477	1012.3863

ψ = 0.35

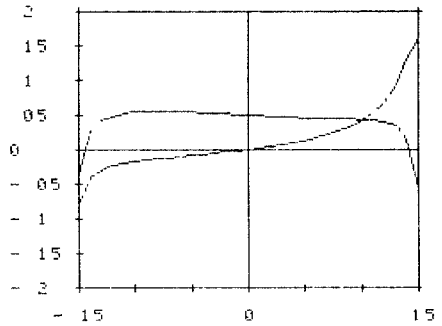

Fig. 5. Frequency response of complex gyrator circuit for second higher order circulation solution with $\kappa = 0.60$, $\psi = 0.450$, and $kR = 2.855$.

where

$$Y_1 \approx \frac{4Y^0}{3} \tag{31}$$

$$Z_1 \approx \frac{(Z^+ + Z^-)}{2} + j\sqrt{3}\,\frac{(Z^+ - Z^-)}{2}. \tag{32}$$

K	KR	G	B'	Q
0.4075	3.4455	0.0010	1.0004	1033.2211
0.4250	3.4363	0.0234	0.8962	38.2293
0.4500	3.4076	0.0562	0.7483	13.3034
0.4750	3.3592	0.0842	0.6302	7.4887
0.5000	3.2948	0.1040	0.5470	5.2578
0.5250	3.2191	0.1168	0.4879	4.1777
0.5500	3.1356	0.1244	0.4436	3.5654
0.5750	3.0464	0.1285	0.4083	3.1761
0.6000	2.9524	0.1301	0.3780	2.9052
0.6250	2.8540	0.1296	0.3503	2.7029
0.6500	2.7510	0.1270	0.3230	2.5433
0.6750	2.6429	0.1216	0.2941	2.4196
0.7000	2.5291	0.1111	0.2657	2.3923
0.7250	2.4116	0.0880	0.2933	3.3339
0.7500	2.3190	0.0345	1.1352	32.8578
0.7625	2.3004	0.0017	2.4187	1444.6155

ψ = 0.1

K	KR	G	B'	Q
0.4075	3.4454	0.0005	0.5265	992.0298
0.4250	3.4354	0.0126	0.4747	37.5908
0.4500	3.4044	0.0303	0.4005	13.2208
0.4750	3.3537	0.0453	0.3405	7.5195
0.5000	3.2871	0.0561	0.2960	5.2814
0.5250	3.2095	0.0631	0.2631	4.1698
0.5500	3.1243	0.0674	0.2377	3.5259
0.5750	3.0334	0.0698	0.2172	3.1099
0.6000	2.9380	0.0709	0.1999	2.8210
0.6250	2.8384	0.0707	0.1844	2.6104
0.6500	2.7347	0.0692	0.1702	2.4594
0.6750	2.6267	0.0660	0.1571	2.3800
0.7000	2.5147	0.0597	0.1494	2.5034
0.7250	2.4031	0.0462	0.1874	4.0531
0.7500	2.3190	0.0181	0.6057	33.4755
0.7625	2.3005	0.0009	1.1783	1288.0047

ψ = 0.2

This network is the dual of the preceding one and may also be arranged to display a frequency response akin to that of a conventional quarter-wave coupled device.

The filter prototype in Fig. 8 may be adjusted to exhibit a Chebyshev frequency response provided the following relationships are satisfied [14]:

$$Q_p = \frac{\sqrt{2}\,(S(\max)-1)^{1/2}}{W} \tag{33}$$

$$Q_s = S(\max)\cdot Q_p \tag{34}$$

$$g = \frac{1}{S(\max)} \tag{35}$$

$$S(\min) = 1.0.$$

g is the normalized gyrator conductance, Q_s and Q_p are the loaded Q-factors of the series and shunt resonators in Fig. 8.

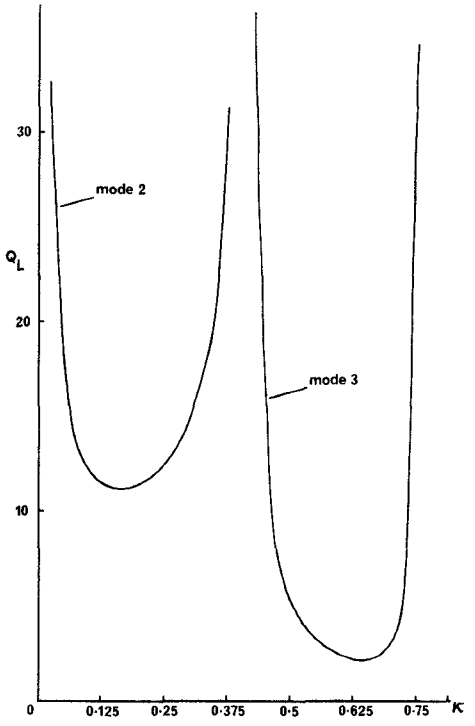

Fig. 6. Loaded Q-factors for first two higher order solutions of junction circulator using disk resonator for $\psi = 0.35$.

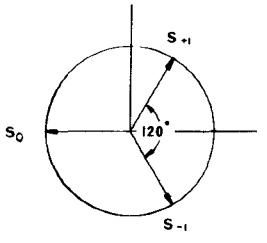

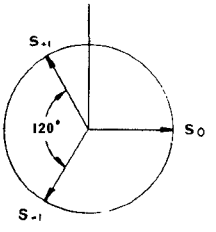

Fig. 7. Eigenvalue diagrams of junction circulators with $s_0 = +1$ and -1.

Taking the value of Q_L used in the example for the second-order solution leads to the following network variables for the device:

$$S(\max) = 1.20$$
$$W = 0.050$$
$$Q_p = 12.60$$
$$Q_s = 15.10$$
$$g = 0.83 \ (G \approx 0.017).$$

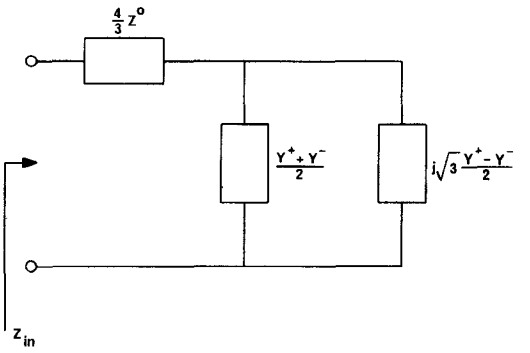

Fig. 8. Complex gyrator circuit of junction circulator with $s_0 = -1$.

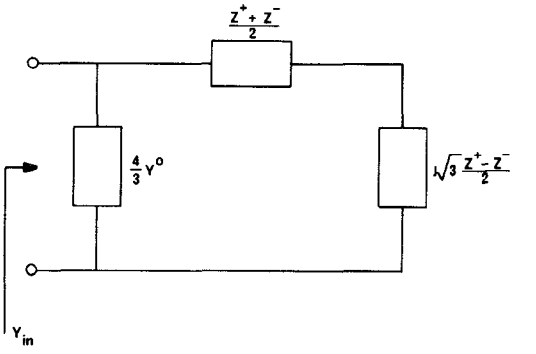

Fig. 9. Complex gyrator circuit of junction circulator with $s_0 = +1$.

This solution displays a similar frequency response to that of the quarter-wave coupled device employing the first higher order solution in a disk resonator, but with a more realizable impedance level for the junction.

VI. Three-Resonant Mode Circulator Using Higher Order Modes in Planar Irregular Hexagonal Resonator

The network topologies of junction circulators using commensurate eigennetworks have been discussed in the previous section, but their practical adjustments have not yet been discussed [8]–[11]. Such circulators require a degeneracy between the in-phase and demagnetized counter-rotating modes. One such natural degeneracy is encountered between the limit $TM_{2,0,-2}$ and $TM_{1,1,-2}$ modes in an irregular hexagonal resonator. This solution is particularly attractive for the construction of circulators at very high frequencies, in that it relies on an oversized resonator for its operation. The design of the circulator discussed here is based on the mode chart in [12], which indicates that the $TM_{2,0,-2}$ and $TM_{1,1,-2}$ limit modes in an oversized irregular hexagonal planar resonator are degenerate. Fig. 10 displays the frequency response of one experimental device using such a resonator. This circulator employed an irregular-hexagonal junction directly coupled to 50-Ω lines. The dimensions of this resonator corresponded to the intersection of the $TM_{2,0,-2}$- and $TM_{1,1,-2}$-limit modes in the irregular hexagonal resonator depicted in Fig. 11 with $kr \approx 3.90$, $\phi \approx 26°$, and $\theta \approx 94°$. The coupling angle (ψ) between the resonator and the uniform lines was as $\psi \approx 13°$

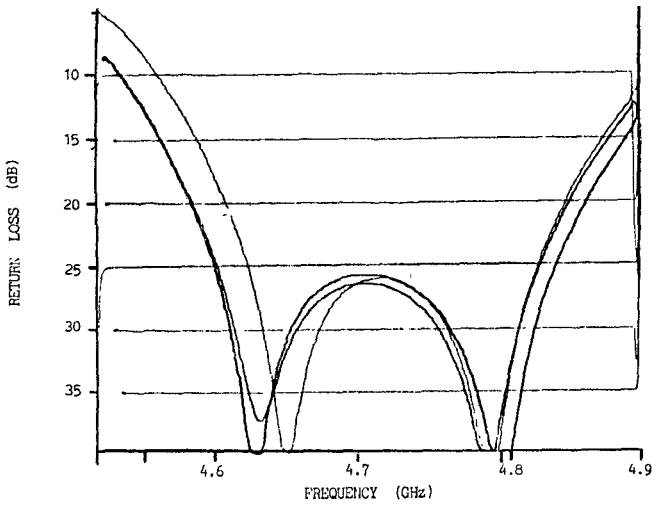

Fig. 10. Frequency response of junction circulator using magnetized planar irregular resonator.

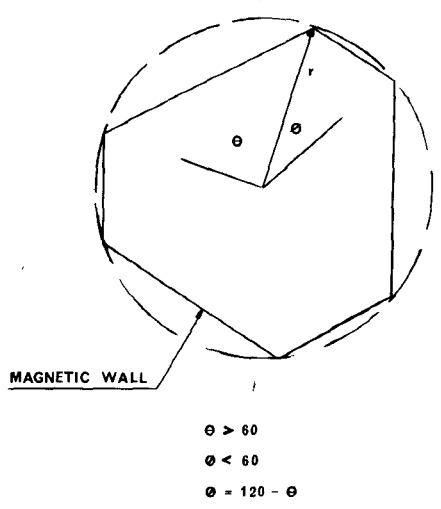

Fig. 11. Schematic diagram of irregular hexagonal resonator.

and the magnetization of the garnet material was 0.0500 T. The experimental bandwidth of the device was about 5 percent at the 25-dB points. Since the loaded Q-factors of the $TM_{2,0,-2}$ and $TM_{1,1,-2}$ modes are not known at this time, no correlation between theory and measurement is possible. However, the experimental bandwidth is consistent with the values of loaded Q-factor exhibited by the second-order solutions in Table I in the case of a disk, and by the values used in the example in the previous section. A similar response has been experimentally obtained in [10].

Consideration of the eigenvalue diagrams of circulators with $s_0 = -1$ and $+1$ in Fig. 7 indicates that the angle between the degenerate eigenvalues in the case $s_0 = +1$ (three resonant mode circulator) is twice the value necessary to realize the eigenvalue diagram for which $s_0 = -1$ (two resonant mode circulator). However, in the conventional situation, the magnetization required to split a dominant pair of modes is twice that necessary to remove the degeneracy between a pair of second-order modes, so that the magnetization required to achieve the three resonant mode solution in Fig. 7 (using a pair of second-order modes) is ideally equal to that necessary to realize a conventional device (using a pair of first-order modes).

VII. Conclusions

The use of resonators employing higher order modes is often an attractive solution to the development of millimeter-wave junction devices. A detailed study of the complex gyrator immittances of the first two higher order solutions of junction circulators using disk resonators indicates that the loaded Q-factor of the first such solution is incompatible with the synthesis of quarter-wave coupled circulators, but that the second one exhibits useful equivalent circuits. A circuit topology that displays a frequency characteristic akin to that of a quarter-wave coupled junction is one in which the in-phase eigennetwork is separately tuned to the frequency of the counter-rotating degenerate ones. One such degeneracy is met in an irregular hexagonal resonator between the in-phase limit $TM_{2,0,-2}$ mode and second-order counter-rotating limit $TM_{1,1,-2}$ ones.

Acknowledgment

The author would like to thank Dr. W. T. Nisbet, Ferranti Ltd., Dundee, Scotland for the experimental work described in this paper.

References

[1] J. B. Davies and P. Cohen, "Theoretical design of symmetrical junction stripline circulators," *IEEE Trans. Microwave Theory Tech.*, vol. MTT-11, pp. 117–123, Mar. 1963.
[2] C. E. Fay and R. L. Comstock, "Operation of the ferrite junction circulator," *IEEE Trans. Microwave Theory Tech.*, vol. MTT-13, pp. 15–27, 1965.
[3] K. Whiting, "Design data for UHF circulators," *IEEE Trans. Microwave Theory Tech.*, vol. MTT-15, pp. 195–198, Mar. 1967.
[4] J. Helszajn, "Quarter-wave coupled junction circulators using weakly magnetized disk resonators," *IEEE Trans. Microwave Theory Tech.*, vol. MTT-30, pp. 800–806, May 1982.
[5] L. K. Anderson, "An analysis of broadband circulators with external tuning elements," *IEEE Trans. Microwave Theory Tech.*, vol. MTT-15, pp. 42–47, Jan. 1967.
[6] J. Helszajn, "The synthesis of quarter-wave coupled circulators with Chebyshev characteristics," *IEEE Trans. Microwave Theory Tech.*, vol. MTT-20, pp. 764–769, Nov. 1972.
[7] R. Levy and J. Helszajn, "Specific equations for one and two section quarter-wave matching networks for stub-resistor loads," *IEEE Trans. Microwave Theory Tech.*, vol. MTT-30, pp. 57–62, Jan. 1982.
[8] Y. Konishi, "A high power u.h.f. circulator", *IEEE Trans. Microwave Theory Tech.*, vol. MTT-15, pp. 700–8, Dec. 1967.
[9] J. Helszajn, "Wideband circulator adjustment using $n = \pm 1$ and $n = 0$ electromagnetic-field patterns," *Electron. Lett.*, vol. 6, pp. 729–31, Nov. 12, 1970.
[10] J. Helszajn, "Three-resonant mode adjustment of the waveguide, circulator," *Radio and Electron. Eng.*, vol. 42, pp. 1–4, Apr. 1972.
[11] Y. Akaiwa, *Electron. Lett.*, vol. 9, no. 12, June 1973.
[12] J. Helszajn, "Standing wave solution of planar irregular and hexagonal resonators," *IEEE Trans. Microwave Theory Tech.*, vol. MTT-29, June 1981.
[13] J. Helszajn, "Operation of tracking circulator," *IEEE Trans. Microwave Theory Tech.*, vol. MTT-29, July 1981.
[14] J. Helszajn and F. M. Aitken, "UHF techniques for lumped element circulators," *Electron. Eng.*, Nov., 1973.

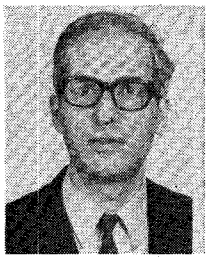

Joseph Helszajn (M'64) was born in Brussels, Belgium, in 1934. He received the Full Technological Certificate of the City and Guilds of London Institute from Northern Polytechnic, London, England in 1955, the M.S.E.E. degree from the University of Santa Clara, Santa Clara, CA, in 1964, the Ph.D. degree from the University of Leeds, Leeds, England, in 1969, and the D.Sc. degree from Heriot-Watt University, Edinburgh, Scotland, in 1976.

He has held a number of positions in the microwave industry. From 1964 to 1966, he was Product Line Manager at Microwave Associates, Inc., Burlington, MA. He is Professor of Microwave Engineering at Heriot-Watt University. He is the author of the books *Principles of Microwave Ferrite Engineering* (New York; Wiley, 1969), *Nonreciprocal Microwave Junctions and Circulators* (New York: Wiley, 1975), and *Passive and Active Microwave Circuits* (New York: Wiley, 1978).

Dr. Helszajn is a Fellow of the Institution of Electronic and Radio Engineers (England). In 1968, he was awarded the Insignia Award of the City and Guilds of London Institute, and a Fellow of the Institute of Electrical Engineers. He is an Honorary Editor of *Microwaves, Optics and Antennas* (IEE Proceedings).

Short Papers

Rectangular Waveguide with Two Double Ridges

D. DASGUPTA AND P. K. SAHA

Abstract—**An eigenvalue equation of a general structure having two arbitrary double ridges in a rectangular waveguide is derived. The cutoff wavelengths of two special cases with two symmetrically placed identical double ridges is computed numerically and their bandwidths are compared. The numerical solution of the eigenvector is also discussed and utilized in determining the gap impedance. As an example of the applications of such ridged waveguides, two varactor-tuned Gunn oscillators are briefly reported.**

I. Introduction

Recently, the authors presented an analysis based on Montgomery's work [1] for determining the eigenvalue spectrum of a rectangular waveguide with two symmetrically placed identical double ridges [2]. The numerical results indicated that such a waveguide would have adequate bandwidth for application in solid-state microwave oscillators. This structure can be generalized by considering two different double ridges at arbitrary locations in the waveguide. The structure treated in [2], [3] is then a special case of this general configuration. Another special case results when one of the two identical double ridges is inverted with respect to the other. The calculations show that the latter structure has a larger bandwidth compared to the former. In addition, some results on the calculation of the gap impedance are also presented. Following the analysis given in [2], we present only the final matrix eigenvalue equations without going into details.

Manuscript received December 29, 1982; revised June 1, 1983.

The authors are with the Institute of Radiophysics and Electronics, Calcutta 700 009, India.

II. Ridged Waveguide

The generalized double-ridged waveguide structure is shown in Fig. 1(a). Two special cases, shown in Figs. 1(b) and 1(c), are referred to as "regular" and "inverted" structures, respectively.

III. Theory

A. Matrix Eigenvalue Equation

To solve the integral eigenvalue equation for TE modes by the Ritz–Galerkin technique, the transverse electric field at the kth aperture of the jth ridge ($j, k = 1,2$) is expanded as

$$E_{j,k}(y) = \sum_{i=0}^{N_{jk}} C_i^{(j,k)} \cos \frac{i\pi}{d_j}(y - h_j). \tag{1}$$

The resulting matrix equation for the eigenvalue k_c then takes the form

$$[H(k_c)]\boldsymbol{C} = 0. \tag{2}$$

The vector $\boldsymbol{C}$ in (2) is given by

$$\boldsymbol{C} = [\boldsymbol{C}^{(1,1)T}\boldsymbol{C}^{(1,2)T}\boldsymbol{C}^{(2,1)T}\boldsymbol{C}^{(2,2)T}]^T \tag{3}$$

where the superscript T denotes the transpose, $[H]$ is a matrix having the following partitioned form:

$$[H] = \begin{bmatrix} H_1 & H_2 & 0 & 0 \\ H_2 & H_3 & H_4 & 0 \\ 0 & H_5 & H_6 & H_7 \\ 0 & 0 & H_7 & H_8 \end{bmatrix}. \tag{4}$$

The eigenvalue equation is then

$$\det[H(k_c)] = 0. \tag{5}$$

0018-9480/83/1100-0938$01.00 ©1983 IEEE